Journal of Biomechanics 84 (2019) 73–80

Contents lists available at ScienceDirect

Journal of Biomechanics

journal homepage: www.elsevier.com/locate/jbiomech
www.JBiomech.com

Agreement of measured and calculated muscle activity during highly dynamic movements modelled with a spherical knee joint

Thomas Dupré *, Mareike Dietzsch, Igor Komnik, Wolfgang Potthast, Sina David

Institute of Biomechanics and Orthopaedics, German Sport University Cologne, Am Sportpark Müngersdorf 6, 50933 Cologne, Germany

ARTICLE INFO

Article history:
Accepted 10 December 2018

Keywords:
AnyBody
Static optimization
EMG
Cutting
Sprinting

ABSTRACT

The inclusion of muscle forces into the analysis of joint contact forces has improved their accuracy. But it has not been validated if such force and activity calculations are valid during highly dynamic multidirectional movements. The purpose of this study was to validate calculated muscle activation of a lower extremity model with a spherical knee joint for running, sprinting and 90°-cutting. Kinematics, kinetics and lower limb muscle activation of ten participants were investigated in a 3D motion capture setup including EMG. A lower extremity rigid body model was used to calculate the activation of these muscles with an inverse dynamics approach and a cubic cost function. Correlation coefficients were calculated to compare measured and calculated activation. The results showed good correlation of the modelled and calculated data with a few exceptions. The highest average correlations were found during walking ($r = 0.81$) and the lowest during cutting ($r = 0.57$). Tibialis anterior had the lowest average correlation ($r = 0.33$) over all movements while gastrocnemius medius had the highest correlation ($r = 0.9$). The implementation of a spherical knee joint increased the agreement between measured and modelled activation compared to studies using a hinge joint knee. Although some stabilizing muscles showed low correlations during dynamic movements, the investigated model calculates muscle activity sufficiently.

1. Introduction

The knowledge about muscle forces and activations, as well as joint forces and moments gives important insights into biomechanical aspects of statics and dynamics of the human body. Information on this is particularly relevant in the field of rehabilitation, injury prevention and athletic performance (Bergmann et al., 1993; Huang and Ferris, 2012; Baum and Li, 2003; David et al., 2017). This applies especially to studies investigating possible injury mechanisms during highly dynamic and multidirectional movements. Studies have identified different muscle activation patterns during cutting manoeuvres (Beaulieu et al., 2009). Such knowledge on the underlying muscle activation patterns is of high importance for the prevention of injuries. Additionally, muscle contraction is, next to the external moments, one part of joint loading in terms of contact forces and joint moments. Thus, a common method to analyse joint forces and moments is the inverse dynamic approach using musculoskeletal models. The inclusion of muscle forces to inverse dynamics calculations is considering the role of the muscle contraction in producing joint load, which is otherwise underestimated (Buchanan et al., 2004).

Inverse dynamics enable the calculation of muscle forces during fundamental activities like walking and more dynamic tasks including running, sprinting and cutting manoeuvres (Besier et al., 2009; Schache et al., 2010). While it is possible to calculate muscle activations and forces involved in any movement in general, there are complications that have to be acknowledged: In principle, only one muscle is needed to move a joint with one degree of freedom. But the human body uses a redundant system of muscles whereby it is statically overdeterminate, leaving an infinite number of solutions to the distribution of the forces (Tsirakos et al., 1997; van Bolhuis and Gielen, 1999). Therefore, modelling of muscle forces has been approached as a minimization problem, where the muscles' forces needed to stabilize the external joint forces, have to be minimized for each involved muscle. Several approaches have been established that specify how the minimized load should be shared between muscles, known as muscle recruitment criterion (Rasmussen et al., 2001; Erdemir et al., 2007; Crowninshield and Brand, 1981; Tsirakos et al., 1997) or cost function henceforth.

* Corresponding author.
E-mail address: t.dupre@dshs-koeln.de (T. Dupré).

https://doi.org/10.1016/j.jbiomech.2018.12.013
0021-9290/

Several studies aimed to compare measured with calculated muscle activity (Pontonnier et al., 2014; Dubowsky et al., 2008; de Zee et al., 2007; Duprey et al., 2015). A sufficient level of agreement between modelled and measured activation for walking, ramp negotiation, one-legged forward jumping and side jumping has been reported (Alexander and Schwameder, 2016; Wibawa et al., 2016). More dynamic movements like cutting have not yet been validated although it is one of the most frequently used movements during team sports and one of the major drivers for anterior cruciate ligament (ACL) injuries. Having a valid musculoskeletal model improves the validity of joint loading and may lead to a better understanding of the underlying activation patterns and their role in ACL ruptures.

Furthermore, previous studies investigated a model in which the knee joint is modelled as a hinge joint. During multi-directional movements, the joint forces and moments, that act in the knee's frontal and transverse plane are important contributors to injury risk (McLean et al., 2004). Therefore, a more sophisticated knee joint model with additional degrees of freedom is needed (Andersen and Rasmussen, 2011), which should provide a more precise modelling of joint moments and muscle forces. Such a model has been validated regarding joint contact forces against data from an instrumented knee prosthesis and showed good results (Richards et al., 2018). They also reported the estimated and measured muscle activity (Richards et al., 2018). However, this was only done for walking and none of the above mentioned studies investigated highly dynamic movements.

This study aims to clarify to what extent the applied model is capable of calculating sufficiently valid muscle activities during such movements. Therefore, muscle activation was calculated by using a model with a spherical knee joint and compared to the results of EMG measurements during highly dynamic multidirectional movements. A high agreement is of importance as muscle activation is a significant factor of joint loading in inverse dynamics calculations.

2. Methods

To validate the lower extremity model, measured electromyography (EMG) data was compared to the activation calculated by the model. Activation levels of eight lower extremity muscles were measured with EMG. Four movements, walking, running, sprinting and 90°-cutting were analysed with a motion capture system. This data was used to calculate muscle activation for the eight measured muscles.

2.1. Participants

Ten male, sportive and healthy participants (75.2 ± 7.5 kg, 181 ± 8 cm) were recruited. Exclusion criteria were acute or chronic injuries of the lower extremity. Each participant gave his written consent for voluntary participation. The study was designed according to the requirements of the Declaration of Helsinki and was approved by the universities ethics commission (Nr. 010/2017).

2.2. Data collection

3D-Kinematic data were collected with a twelve camera motion capture system (200 Hz, Vicon, Oxford, UK). One force plate (1000 Hz, Kistler, Winterthur, CH) was embedded in the floor to record ground reaction forces. Fifty-two markers were attached to the participants' skin by means of ph-neutral, double-sided, adhesive tape. Segment length' and circumferences of each participant were measured to be incorporated into the modelling process later on. EMG-electrodes were attached according to the SENIAM recommendations (Hermens et al., 1999) to record muscle activity of the following eight muscles: gluteus medius, vastus medialis, vastus lateralis, biceps femoris caput longum, semitendinosus, gastrocnemius, soleus and tibialis anterior of the right, dominant leg. Muscle activity was recorded with a wireless system (1000 Hz, myon, Schwarzenberg, CH). Prior to the measurement the participants were instructed to warm up individually.

Each participant had to perform five valid trials of each of the following testing conditions in a randomized order: walking (W), running (R), sprinting (S) and 90°-cutting (C). A trial was valid if the participant had clear contact to the force plate with his right foot. For W and R, the participants had to stay in a velocity range of $1.7\ \mathrm{m\,s^{-1}} \pm 5\%$ and $4.0\ \mathrm{m\,s^{-1}} \pm 5\%$, respectively, which was controlled by the use of photoelectric sensors. S was performed as a full effort sprint start, where the fourth ground contact after the start was recorded on the force plate. The speed measured as average centre of mass speed during force plate contact was $6.4 \pm 0.25\ \mathrm{m\,s^{-1}}$. During C, participants had to perform a 90°-cutting manoeuvre as can be seen in Fig. 1. They were instructed to perform the manoeuvre as fast as possible without a specified approach velocity. Their dominant right leg had to be placed on the force plate (Fig. 1).

2.3. Modelling

A modified version of the Anatomical Landmark Scaled Model (Lund et al., 2015) (seven segments, nine degrees of freedom) in AnyBody Modelling System was used. This model maps the musculoskeletal model template to a subject specific scaled stickfigure (Lund et al., 2015). Anatomic parameters of the model are based on a cadaveric study by Klein Horsman et al. (2007) and the segment masses were calculated as described by Hanavan (1964) from the measured segment parameters. The knee was modelled as a spherical knee joint with three degrees of freedom instead of using a hinge joint as in the original model. The hip joint was modelled as a spherical joint as well while the talocalcaneal and subtalar joints were each modelled as hinge joints. Kinematic and kinetic data were low-pass filtered using a recursive 2nd order Butterworth filter with a cut-off frequency of 6 Hz in the gait trials and 20 Hz for the other conditions. Joint angles calculated from motion capture data and ground reaction forces were used as input for an inverse dynamics analysis. The ligaments of the knee were simulated by providing the kneemodel with reaction moments that constrained movement in the frontal and transversal plane (Richards et al.,

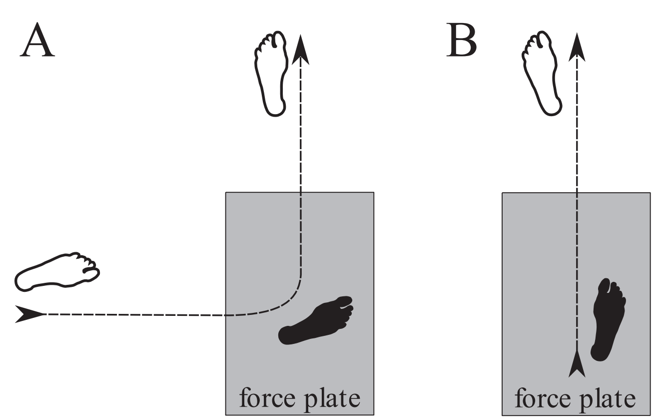

Fig. 1. Schematic drawing of the force plate setup for the cutting manoeuvre (A) and the other three movement conditions (B). The black foot print indicates the force plate contact that was analysed in the present study. Movement direction is indicated by the black arrow.

Table 1
Number of mean EMG-signals of a specific muscle, that had to be excluded due to exceeding two times the standard deviation of the cohorts' muscles' mean.

Muscle	Walking	Running	Sprinting	Cutting
Gluteus medius	5	3	2	4
Vastus medialis	4	2	3	4
Vastus lateralis	3	2	3	2
Biceps femoris	3	1	2	3
Semimembranosus	3	2	2	2
Soleus	3	4	3	1
Gastrocnemius medialis	3	2	1	2
Tibialis anterior	3	2	2	2

2018). To distribute the net joint moments to the muscles, the 'AnyMuscleModel', a hill type muscle model with static optimization and a cubic cost function, was used. It relies only on the maximum isometric strength $F_{\max}$ of the muscle, which is derived from its scaled physiological cross sectional area. From this, muscle activation is calculated as $\frac{F_M}{F_{\max}}$ with F_M being the current force (Rasmussen et al., 2001). The same model has already been validated regarding knee contact forces during walking (Richards et al., 2018).

For muscles with numerous substrands as described by van der Helm and Veenbaas (1991), calculated activity was reduced to the envelope of all substrands by choosing the maximum value of all parts for each point in time. Functional differences of muscle parts, as in the posterior and anterior parts of gluteus medius, were not considered as they are not measurable with surface EMG due to cross-talk. The exception to this was the biceps femoris. Only its caput longum was analysed, as its caput breve is covered by other muscles.

2.4. Data processing

Data processing was done in Matlab 2017a (The MathWorks, Natick, Massachusetts, USA). Raw EMG-data was band-pass filtered with a 2nd order Butterworth filter with cut-off frequencies of 20 and 400 Hz. Afterwards, the linear envelope of the EMG-data was extracted with a 4th order Butterworth low-pass filter at 6 Hz cut-off frequency.

It has been shown, that there is a delay between the onset of muscle activation and the onset of force production in a muscle (Cavanagh and Komi, 1979; Norman and Komi, 1979), called electromechanical delay (EMD). Because modelled activation is calculated from ground reaction forces, EMD had to be accounted for. EMD varies between 10 and 100 ms, depending on the investigated muscle and contraction mode (Begovic et al., 2014). An EMD of 40 ms has been found for voluntary contractions of the thigh muscles (Zhou et al., 1995). Therefore, measured activation was right shifted by 40 ms.

EMG and modelled activation was normalized separately for each trial. The measured and modelled activation was normalized according to the peak dynamic activity method (Sinclair et al., 2015). Therefore the peak activation of all condition trials was determined and used for normalization. The single trials are then expressed as % activation relative to the peak activation during this condition and each participant. Trials were also time normalized to force plate contact with touch down being 0% and toe-off 100%. Means for measured and estimated activation were calculated for each condition and muscle. Mean EMG-signals of each muscle were excluded if they deviated by more than two standard deviations from the cohorts' muscles' overall mean.

The two signals' similarity was investigated by calculating the Pearson correlation coefficient (CC) between measured and calculated activation for all data points of the mean curves of each muscle in each movement condition and expressed as CC but also R^2 values. The recommendations made by Cohen (1988) were used to classify CC as poor ($r = 0.1–0.29$), moderate ($r = 0.3–0.49$) and strong ($r = 0.5–1$) correlations. Average CC (avCC) was calculated for every movement and muscle.

3. Results

In 83 cases muscles had to be excluded from the analysis which was 20.8% of all means (Table 1). Of the calculated CCs, 75% showed a strong correlation, 12.5% showed a moderate correlation and 12.5% showed a poor correlation (Table 2). Gluteus medius and Soleus (during R) showed the highest correlation with a CC of 0.98. The lowest CC was found in m. biceps femoris during R (-0.59). Comparing the avCC from all muscles between the movements, W had the highest avCC with 0.81. S showed the second highest avCC with 0.69 whereas R had an avCC of 0.64 and C had the lowest avCC with 0.57. From the perspective of the individual muscles over all four conditions, the highest avCC was found for gastrocnemius medius (0.9) while the lowest avCC was found in tibialis anterior (0.33). Muscle activation, including the standard deviations, increased in the dynamic conditions compared to W. Fig. 2 shows the mean activation curves of all muscles in the four conditions. As the calculated muscle activation is related on the joint moments and reaction forces, the knee joint moments and reaction forces of the spherical knee joint are reported in Appendices A and B.

4. Discussion

The aim of this study was to compare calculated muscle activity with the muscle activity measured by means of EMG during highly dynamic movement tasks in respect to the usage of a spherical knee joint model. In this regard, strong correlations between the modelled and measured muscle activation were found in most conditions and muscles. These results show, that the applied model can satisfactorily estimate muscle activation patterns not only during W but also during multidirectional, highly dynamic movements like C. Time series of measured activation patterns are similar to those previously published for level walking (Hof et al., 2005; Alexander and Schwameder, 2016; Huang and Ferris, 2012; Winter and Yack, 1987) and running (Gazendam and Hof, 2007). Calculated activations of the gait trials are also similar to previously published patterns (Alexander and Schwameder, 2016; Ding et al., 2016; Modenese and Phillips, 2012). Activation patterns for S are comparable to the study of Jacobs and van Ingen Schenau (1992), although a different step was analysed and the chosen shift to account for EMD was longer.

To the authors knowledge, no articles exist showing time series for EMG-measurements during a 90°-cutting manoeuvre. However, the presentation of time series gives interesting insights which cannot be given by reporting peak values or integrals. It allows to relate the acting net moments to the muscle activation

Table 2
CCs from the averaged trials of the ten participants in the four conditions. Numbers in brackets represent the associated R^2 value. Correlations were calculated for an EMD of 40 ms.

Muscle	Walking	Running	Sprinting	Cutting
Gluteus medius	0.23 (0.05)	0.98 (0.96)	0.77 (0.59)	0.58 (0.34)
Vastus medialis	0.84 (0.71)	0.93 (0.86)	0.96 (0.92)	0.75 (0.56)
Vastus lateralis	0.87 (0.76)	0.92 (0.85)	0.95 (0.90)	0.76 (0.58)
Biceps femoris	0.9 (0.81)	−0.59 (0.35)	0.92 (0.85)	0.3 (0.09)
Semimembranosus	0.75 (0.56)	0.38 (0.14)	0.96 (0.92)	0.46 (0.21)
Soleus	0.97 (0.94)	0.98 (0.96)	0.47 (0.22)	0.64 (0.41)
Gastrocnemius medialis	0.95 (0.90)	0.89 (0.79)	0.87 (0.76)	0.9 (0.81)
Tibialis anterior	0.97 (0.94)	0.62 (0.38)	−0.42 (0.18)	0.16 (0.03)

and therefore understand the strength and weakness of the used approach. As C is the only one of the four movement conditions that requires a change of direction it is reasonable that the standard deviation of the mean activation is higher than in the other conditions (Fig. 2). Due to the less restricted movement path during C, participants are allowed more individual movement and activation patterns leading to a higher standard deviation (David et al., 2017).

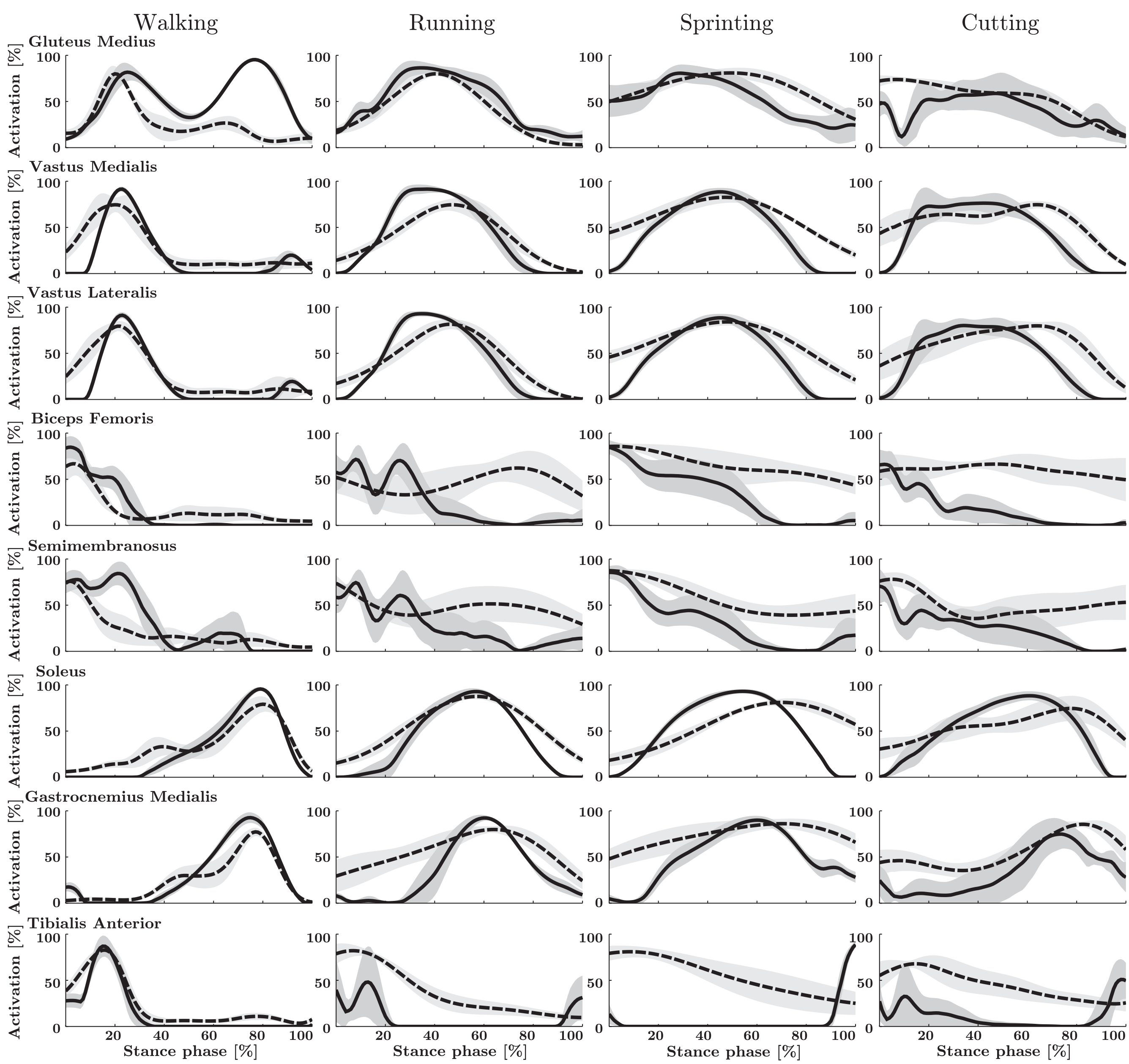

Fig. 2. Time series from ten participants for the relative activation (100% = maximum activation of specific movement condition) of the eight investigated muscles during force plate contact for each movement condition. Solid lines are measured activation and dashed lines show calculated activation. Shaded areas indicate the standard deviation. Curves are time-normalized to force plate contact.

Using a spherical knee joint is of high interest for future studies on injury mechanisms in ACL tears. The three degrees of freedom of the joint allow for a distribution of joint moments to the non-sagittal plane. It has already been shown, that tibia torsion, which is provoked by rotational knee moments, increases the load on the ACL substantially (Markolf et al., 1995; McLean et al., 2004). Thereby, the rotational and frontal plane torques, important for the investigation of ACL ruptures, can be studied with a higher validity when a spherical knee joint is used. Those moments also add to the required muscle forces leading to more realistic muscle activation curves which is seen by the higher CCs for walking compared to previous studies (Alexander and Schwameder, 2016; Wibawa et al., 2016). Furthermore, a higher number of degrees of freedom at the knee joint has been shown to result in higher joint contact forces in the knee (Cleather and Bull, 2011). Thereby, muscle activity of muscles around the knee joint is underrepresented in models with a hinge joint for a knee model.

Nevertheless, Fig. 2 shows, that several muscles have an underestimated calculated muscle activity, especially shortly after touch down and before toe off. This can be explained by the fact, that the measured activity will never be zero, especially during fast movements where the pre-activation is used by the nervous system (Bencke and Zebis, 2011). Calculated activity can be zero as it only reflects the net joint moments. Furthermore, co-contraction cannot be addressed by static optimization as it is used by AnyBody. The effect is most pronounced in the more dynamic movements where co-contraction is needed to stabilize the joints and therefore accounts for a substantial amount of muscle activity. This could explain the weak CCs of biceps femoris and semimembranosus during R and C where they are likely to be used for stabilization. During S, tibialis anterior shows a negative correlation because the muscle is not needed to create the accelerating extension moment at the ankle joint, but is needed by the nervous system to stabilize the joint. Because stabilizing pre- and co-activation do not increase the net-moments around joints, the modelled activation stays low in the absence of high net-moments. Therefore, the missing co-contraction is the strongest weakness of static optimization, as especially those muscles that have no accelerating but only stabilizing functions in the dynamic movements, show low or even negative CCs. First promising efforts to overcome this issue have been made by using EMG-data to constrain the static optimization with 'co-contraction entropy' to increase co-contraction activity for index finger muscles (MacIntosh and Keir, 2017).

Apart from that, 75% of the CCs showed a strong correlation, proving that the cubic cost-function was an adequate choice for the investigated movement tasks. Gluteus medius during W was one exception where a different cost-function might provide better results: It shows a low correlation during W which is based on to the second peak in its calculated activation (Fig. 3). This peak is not existent in the measured activation which declines fast after the first peak until the end of the stance phase. The same patterns for measured and calculated activation have been shown in a previous study (de Groote et al., 2014). When comparing the corresponding hip joint moments that have to be distributed to the

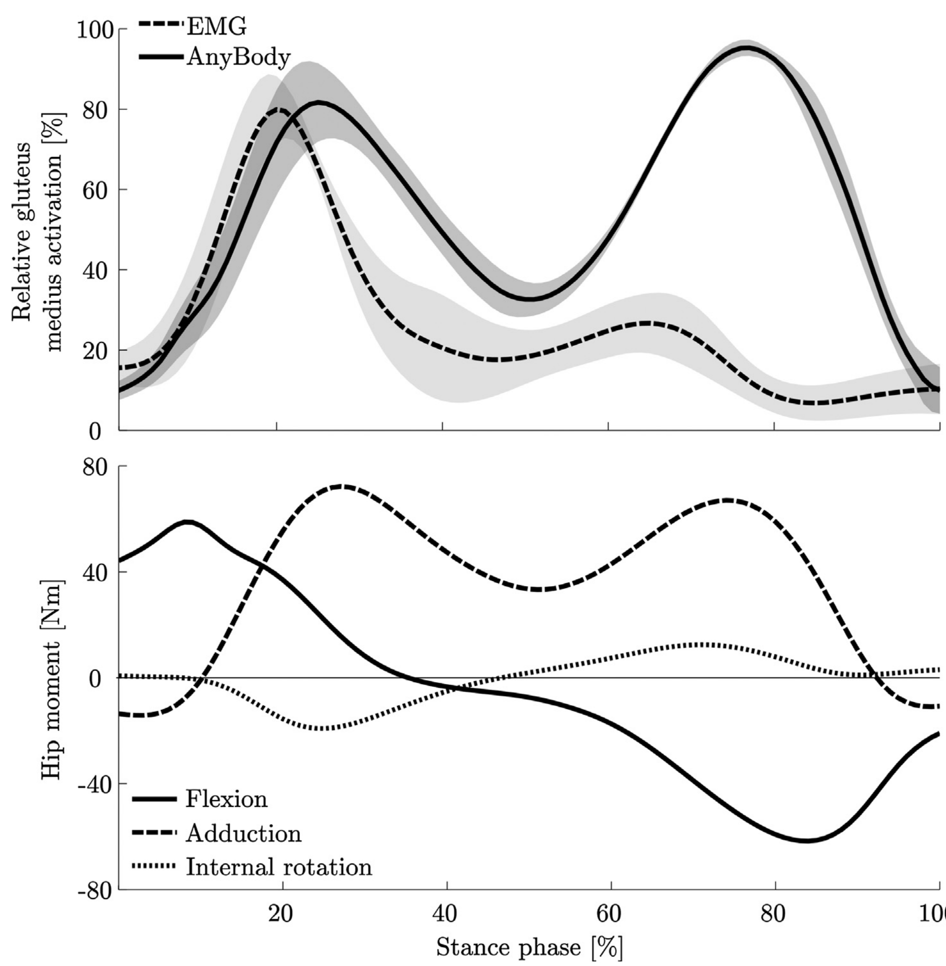

Fig. 3. Time series from ten participants for the relative activation of m. gluteus medius (100% = maximum activation of specific movement condition) during W on top, external hip joint moments at the bottom. Shaded areas indicate the standard deviation of relative activation. Curves are time- normalized to force plate contact.

hip muscles, it is obvious, that the curve of the calculated activation is similar to that of the hip abduction moment (Fig. 3). Therefore, an overestimation of the gluteus medius activation due to the cost function is the most likely explanation to the second peak and hence the low CC. While the external hip adduction moment is countered mostly by the gluteus medius in the model, other abductor muscles might contribute to a higher extend in the real body. Thereby only a small second peak would occur in gluteus medius activation which corresponds to the small peak that is visible in the measured activation at around 70% of stance (Fig. 3).

Previous studies have calculated the mean absolute error (MAE) to investigate the differences in relative activation between calculated and measured activation (Alexander and Schwameder, 2016). Although this can be useful additional information, MAE calculation was omitted in the present study. While EMG measures the electric potential that activates the muscles acting on a joint, the modelled activation describes the distribution of joint moments. The use of the MAE assumes a comparability of the absolute values, which is questionable according to the different sources of data.

The study is limited by the method of investigating the spherical knee joint through muscle activations. Ideally, instrumented knee prostheses would provide joint contact forces that could be compared to the calculated contact forces (Fregly et al., 2012). But participants with artificial knee joints are unlikely to perform the movements of S and C in a way that would be comparable to the average population if they are able to perform them at all. During dynamic movements, soft tissue artefacts can influence the calculation of the joint moments and muscle activation, especially in the non-sagittal movement planes (Camomilla et al., 2017). While the influence was not assessed in this study, the impact on the reported results is suggested to be negligible due to the investigated movement plane. The examined muscles are mainly responsible for sagittal plane movements where the influence of soft tissue artefacts is the lowest (Akbarshahi et al., 2010). Furthermore, their impact is reduced by filtering the marker trajectories before the inverse dynamics calculation. The model in this study used a cubic cost function to distribute the net moments. Although this is thought to work better than a simple quadratic recruitment, no artificial muscle recruitment algorithm can simulate the natural recruitment precisely (Wibawa et al., 2016). The calculation of the maximum stress (Marras and Sommerich, 1991) might improve the comparability of calculated and measured activation but has only been shown for simple mono-planar motions so far. Therefore, the applicability of this approach is limited for highly dynamic multi-planar movements. Lastly, the muscle model ignored important parameters like contraction velocity and current muscle length. While this might have reduced the CC scores, such simple models circumvent making assumptions on muscle parameters needed for more detailed models and are therefore frequently used.

5. Conclusion

The present study has shown, that the use of a spherical knee joint can improve the correlation compared to previous studies that used a hinge joint. Although correlations for more dynamic movements like S and C are lower than in W, they were still as high as in previous studies on walking. Especially for investigating ACL injury risk, using a spherical knee joint should help to understand the role of rotational moments on tibia torsion. However, the results should not be used carelessly as muscles that are used in the body as stabilizing muscles showed only weak correlations due to co-contraction playing a dominant role in the activation levels. But high correlations for the propulsion muscles show a high accuracy in predicting their activation patterns. Therefore, modelling muscle activation can be seen as a valuable tool for understanding these patterns during movements with a high injury risk.

Conflict of interest statement

The authors report no conflicts of interest.

Acknowledgements

Igor Komnik and Sina David received funding from a graduate fellowship of the German Sport University Cologne.

Appendix A

Fig. 4

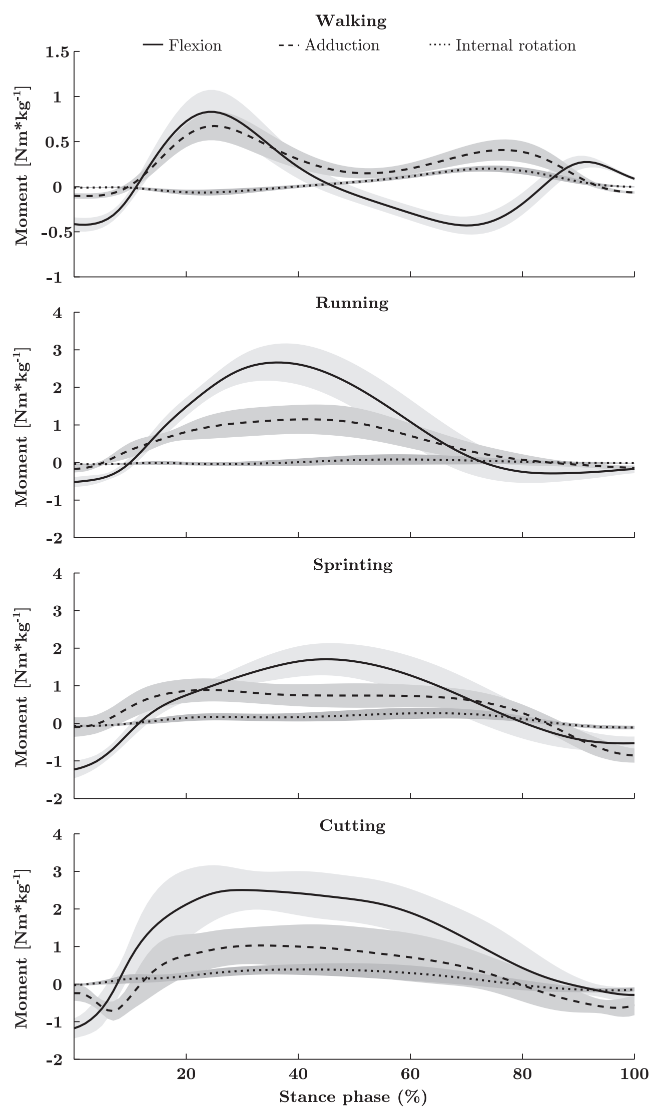

Fig. 4. Time series of the knee joint moments of ten participants in each of the four movement conditions. Joint moments are reported as external moments normalized to body weight and force plate contact. Positive values correspond with the labels of the legend. Lines represent the mean curves while shaded areas represent the standard deviation.

Appendix B

Fig. 5

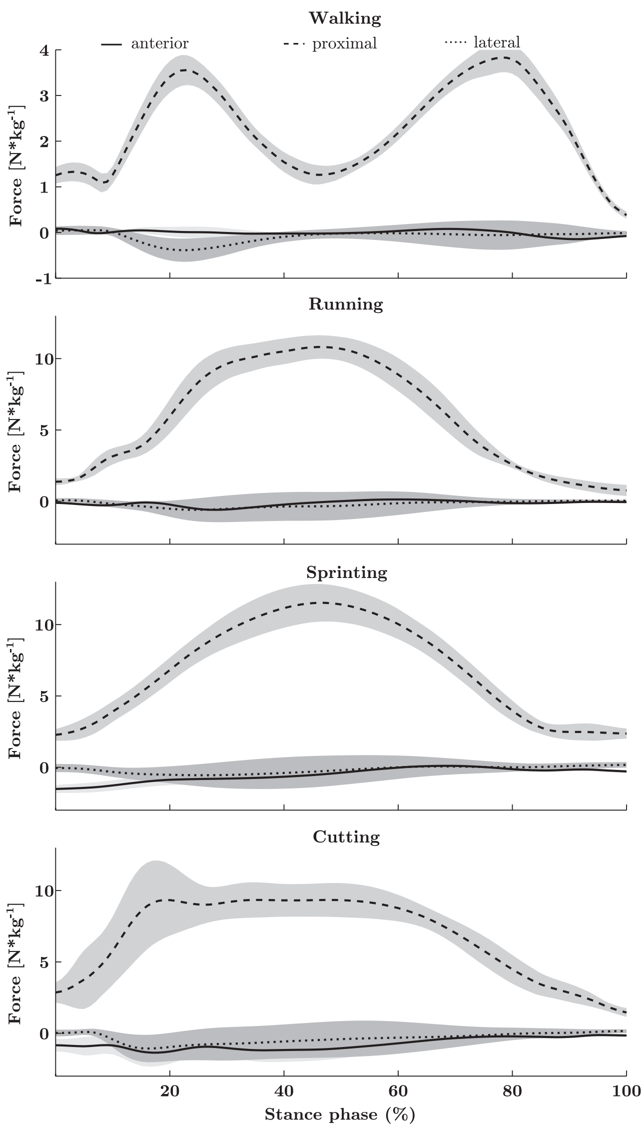

Fig. 5. Time series of the knee joint reaction forces of ten participants in each of the four movement conditions. Joint contact forces are normalized to body weight and force plate contact. Positive values correspond with the labels of the legend. Lines represent the mean curves while shaded areas represent the standard deviation.

References

Akbarshahi, M., Schache, A.G., Fernandez, J.W., Baker, R., Banks, S., Pandy, M.G., 2010. Non-invasive assessment of soft-tissue artifact and its effect on knee joint kinematics during functional activity. J. Biomechanics 43 (7), 1292–1301.

Alexander, N., Schwameder, H., 2016. Comparison of estimated and measured muscle activity during inclined walking. J. Appl. Biomechanics 32 (2), 150–159.

Andersen, M.S., Rasmussen, J., 2011. Total knee replacement musculoskeletal model using a novel simulation method for non-conforming joints. In: Proceedings of the International Society of Biomechanics. ISB, Brussels.

Baum, B.S., Li, L., 2003. Lower extremity muscle activities during cycling are influenced by load and frequency. J. Electromyography Kinesiology: Off. J. Int. Soc. Electrophysiological Kinesiology 13, 181–190.

Beaulieu, M.L., Lamontagne, M., Xu, L., 2009. Lower limb muscle activity and kinematics of an unanticipated cutting manoeuvre: a gender comparison. Knee Surg. Sports Traumatology Arthroscopy 17 (8), 968–976.

Begovic, H., Zhou, G.-Q., Li, T., Wang, Y., Zheng, Y.-P., 2014. Detection of the electromechanical delay and its components during voluntary isometric contraction of the quadriceps femoris muscle. Frontiers Physiol. 5, 1–8.

Bencke, J., Zebis, M.K., 2011. The influence of gender on neuromuscular pre-activity during side-cutting. J. Electromyography Kinesiology: Off. J. Int. Soc. Electrophysiological Kinesiology 21 (2), 371–375.

Bergmann, G., Graichen, F., Rohlmann, A., 1993. Hip joint loading during walking and running, measured in two patients. J. Biomechanics 26 (8), 969–990.

Besier, T.F., Fredericson, M., Gold, G.E., Beaupré, G.S., Delp, S.L., 2009. Knee muscle forces during walking and running in patellofemoral pain patients and pain-free controls. J. Biomechanics 42 (7), 898–905.

Buchanan, T.S., Lloyd, D.G., Manal, K., Besier, T.F., 2004. Neuromusculoskeletal modeling: estimation of muscle forces and joint moments and movements from measurements of neural command. J. Appl. Biomechanics 20 (4), 367–395.

Camomilla, V., Dumas, R., Cappozzo, A., 2017. Human movement analysis: the soft tissue artefact issue. J. Biomechanics 62, 1–4.

Cavanagh, P.R., Komi, P.V., 1979. Electromechanical delay in human skeletal muscle under concentric and eccentric contractions. Eur. J. Appl. Physiol. Occup. Physiol. 42 (3), 159–163.

Cleather, D.J., Bull, A.M., 2011. Knee and hip joint forces-sensitivity to the degrees of freedom classification at the knee. Proc. Inst. Mech. Eng. Part H: J. Eng. Med. 225 (6), 621–626.

Cohen, J., 1988. Statistical Power Analysis for the Behavioral Sciences. Erlbaum, Hillsdale, NJ.

Crowninshield, R.D., Brand, R.A., 1981. A physiologically based criterion of muscle force prediction in locomotion. J. Biomechanics 14 (11), 793–801.

David, S., Komnik, I., Peters, M., Funken, J., Potthast, W., 2017. Identification and risk estimation of movement strategies during cutting maneuvers. J. Sci. Med. Sport 20 (12), 1075–1080.

de Groote, F., Jonkers, I., Duysens, J., 2014. Task constraints and minimization of muscle effort result in a small number of muscle synergies during gait. Front. Comput. Neurosci. 8, 1–11.

de Zee, M., Dalstra, M., Cattaneo, P.M., Rasmussen, J., Svensson, P., Melsen, B., 2007. Validation of a musculo-skeletal model of the mandible and its application to mandibular distraction osteogenesis. J. Biomechanics 40 (6), 1192–1201.

Ding, Z., Nolte, D., Kit Tsang, C., Cleather, D.J., Kedgley, A.E., Bull, A.M.J., 2016. In vivo knee contact force prediction using patient-specific musculoskeletal geometry in a segment-based computational model. J. Biomechanical Eng. 138 (2), 021018.

Dubowsky, S.R., Rasmussen, J., Sisto, S.A., Langrana, N.A., 2008. Validation of a musculoskeletal model of wheelchair propulsion and its application to minimizing shoulder joint forces. J. Biomechanics 41 (14), 2981–2988.

Duprey, S., Savonnet, L., Black, N., Wang, X., 2015. Muscle force prediction: can we rely on musculoskeletal model estimations? a case study on push force exertions with the upper limb. Comput. Methods Biomechanics Biomed. Eng. 18 S1, 1934–1935.

Erdemir, A., McLean, S., Herzog, W., van den Bogert, A.J., 2007. Model-based estimation of muscle forces exerted during movements. Clin. Biomech. 22 (2), 131–154.

Fregly, B.J., Besier, T.F., Lloyd, D.G., Delp, S.L., Banks, S.A., Pandy, M.G., D'Lima, D.D., 2012. Grand challenge competition to predict in vivo knee loads. J. Orthop. Res. 30 (4), 503–513.

Gazendam, M.G., Hof, A.L., 2007. Averaged EMG profiles in jogging and running at different speeds. Gait Posture 25 (4), 604–614.

Hanavan, E.P., 1964. A mathematical model of the human body. Aerospace Medical Research Laboratories, Wright-Patterson Air Force Base, Ohio.

Hermens, H.J., Freriks, B., Merletti, R., Stegeman, D., Blok, J., Rau, G., Disselhorst-Klug, C., Hägg, G., 1999. European recommendations for surface electromyography. Roessingh Res. Dev. 8 (2), 13–54.

Hof, A.L., Elzinga, H., Grimmius, W., Halbertsma, J.P.K., 2005. Detection of non-standard EMG profiles in walking. Gait Posture 21 (2), 171–177.

Huang, S., Ferris, D.P., 2012. Muscle activation patterns during walking from transtibial amputees recorded within the residual limb-prosthetic interface. J. Neuroengineering Rehabilitation 9 (55), 1–16.

Jacobs, R., van Ingen Schenau, G.J., 1992. Intermuscular coordination in a sprint push-off. J. Biomechanics 25 (9), 953–965.

Klein Horsman, M.D., Koopman, H.F.J.M., van der Helm, F.C.T., Poliacu Prosé, L., Veeger, H.E.J., 2007. Morphological muscle and joint parameters for musculoskeletal modelling of the lower extremity. Clin. Biomech. 22 (2), 239–247.

Lund, M.E., Andersen, M.S., de Zee, M., Rasmussen, J., 2015. Scaling of musculoskeletal models from static and dynamic trials. Int. Biomech. 2 (1), 1–11.

MacIntosh, A.R., Keir, P.J., 2017. An open-source model and solution method to predict co-contraction in the finger. Comput. Methods Biomechanics Biomed. Eng. 20 (13), 1373–1381.

Markolf, K.L., Burchfield, D.M., Shapiro, M.M., Shepard, M.F., Finerman, G.A., Slauterbeck, J.L., 1995. Combined knee loading states that generate high anterior cruciate ligament forces. J. Orthop. Res. 13 (6), 930–935.

Marras, W.S., Sommerich, C.M., 1991. A three-dimensional motion model of loads on the lumbar spine: I. Model structure. Human Factors 33 (2), 123–137.

McLean, S.G., Huang, X., Su, A., Van Den Bogert, A.J., 2004. Sagittal plane biomechanics cannot injure the ACL during sidestep cutting. Clin. Biomechanics 19 (8), 828–838.

Modenese, L., Phillips, A.T.M., 2012. Prediction of hip contact forces and muscle activations during walking at different speeds. Multibody Sys. Dyn. 28 (1), 157–168.

Norman, R.W., Komi, P.V., 1979. Electromechanical delay in skeletal muscle under normal movement conditions. Acta Physiol. Scand. 106 (3), 241–248.

Pontonnier, C., de Zee, M., Samani, A., Dumont, G., Madeleine, P., 2014. Strengths and limitations of a musculoskeletal model for an analysis of simulated meat cutting tasks. Appl. Ergonomics 45 (3), 592–600.

Rasmussen, J., Damsgaard, M., Voigt, M., 2001. Muscle recruitment by the min/max criterion – a comparative numerical study. J. Biomechanics 34 (3), 409–415.

Richards, R.E., Andersen, M.S., Harlaar, J., van den Noort, J.C., 2018. Relationship between knee joint contact forces and external knee joint moments in patients with medial knee osteoarthritis: effects of gait modifications. Osteoarthritis Cartilage 26 (9), 1203–1214.

Schache, A.G., Kim, H.-J., Morgan, D.L., Pandy, M.G., 2010. Hamstring muscle forces prior to and immediately following an acute sprinting-related muscle strain injury. Gait Posture 32 (1), 136–140.

Sinclair, J., Taylor, P.J., Hebron, J., Brooks, D., Hurst, H.T., Atkins, S., 2015. The reliability of electromyographic normalization methods for cycling analyses. J. Human Kinet. 46, 19–27.

Tsirakos, D., Baltzopoulos, V., Bartlett, R., 1997. Inverse optimization: functional and physiological considerations related to the force-sharing problem. Crit. Rev. Biomed. Eng. 25 (4-5), 371–407.

van Bolhuis, B.M., Gielen, C., 1999. A comparison of models explaining muscle activation patterns for isometric contractions. Biol. Cybernetics 81 (3), 249–261.

van der Helm, F., Veenbaas, R., 1991. Modelling the mechanical effect of muscles with large attachment sites: application to the shoulder mechanism. J. Biomechanics 24 (12), 1151–1163.

Wibawa, A.D., Verdonschot, N., Halbertsma, J.P.K., Burgerhof, J.G.M., Diercks, R.L., Verkerke, G.J., 2016. Musculoskeletal modeling of human lower limb during normal walking, one-legged forward hopping and side jumping: comparison of measured EMG and predicted muscle activity patterns. J. Biomechanics 49 (15), 3660–3666.

Winter, D.A., Yack, H.J., 1987. EMG profiles during normal human walking: stride-to-stride and inter-subject variability. Electroencephalography Clin. Neurophysiol. 67 (5), 402–411.

Zhou, S., Lawson, D.L., Morrison, W.E., Fairweather, I., 1995. Electromechanical delay in isometric muscle contractions evoked by voluntary, reflex and electrical stimulation. Eur. J. Appl. Physiol. 70 (2), 138–145.